Taylor & Francis
Taylor & Francis Group

Science and Technology for the Built Environment

ISSN: (Print) (Online) Journal homepage: https://www.tandfonline.com/loi/uhvc21

Performance study and life-cycle cost analysis of a ground-source heat-pump system in a commercial building in Norway

Vetle Kjær Risinggård, Ove Sivertsen, Ulrik Thisted & Kirsti MidttØmme

To cite this article: Vetle Kjær Risinggård, Ove Sivertsen, Ulrik Thisted & Kirsti MidttØmme (2022): Performance study and life-cycle cost analysis of a ground-source heat-pump system in a commercial building in Norway, Science and Technology for the Built Environment, DOI: 10.1080/23744731.2022.2097819

To link to this article: https://doi.org/10.1080/23744731.2022.2097819

Published online: 22 Sep 2022.

Science and Technology for the Built Environment, (2022) **0**, 1–15

ISSN: 2374-4731 print / 2374-474X online
DOI: 10.1080/23744731.2022.2097819

Performance study and life-cycle cost analysis of a ground-source heat-pump system in a commercial building in Norway

VETLE KJÆR RISINGGÅRD[1]*, OVE SIVERTSEN[2], ULRIK THISTED[1] and KIRSTI MIDTTØMME[1]

[1]*Energy & Technology, NORCE Norwegian Research Centre AS, Bergen, Norway*
[2]*B. Fondenes AS, Bergen, Norway*

High-performance systems are a prerequisite for profitable borehole thermal-energy storage. This paper presents performance measures for a system operating at a seasonal performance factor of 4.5 and evaluates the life-cycle costs of the actual and alternative system configurations. Compared to systems using dry cooling and electric or district heating the as-built system represents a profitable investment with internal rates of return of respectively 4.9% and 5.9% over a 50-year life cycle. Consequently, ambient-temperature borehole thermal-energy storage is economically competitive in North-European climates at current prices.

Introduction

Buildings consume more than 55% of global electricity production, thus indirectly contributing 20% of global CO_2 emissions (Wörsdörfer et al. 2019). The International Energy Agency indicates that in order to limit the rise in global temperatures to 1.5 °C as outlined by the United Nations Intergovernmental Panel on Climate Change (Masson-Delmotte et al. 2019), all new buildings have to be zero-carbon ready in advanced economies by 2025, and 50% of existing buildings have to be retrofitted to zero-carbon-ready levels by 2040 (Cozzi et al. 2021).

Zero-carbon-ready buildings can be heated and cooled by a range of energy sources, including electricity generated by renewables. However, the extensive electrification required to decarbonize the energy system will strain renewable electricity generation as well as the transmission grid (Cozzi et al. 2021). Even in Norway, which today derives 99% of its electricity production from wind and hydropower (Statistics Norway 2021a), an extensive electrification requires more than a 30% increase in the renewable energy production (Holmefjord and Kringstad 2019). Meeting building heating and cooling needs with on-site utilization of lower-exergy sources such as geothermal heat will ease the load placed on the energy system by electrification.

About 800 ground-source heat pump (GSHP) installations with more than eight borehole heat exchangers (BHE) have been installed in Norway the last three decades (Midttømme et al. 2021). Traditionally, these systems have been designed for heating. Many large GSHP systems for multi-family houses are still designed only for heating purposes, but the share of borehole thermal-energy storages (BTES) used for both heating and cooling is increasing. Several of the new installations are integrated systems combining solar energy and BTES (Midttømme et al. 2008, 2021). Performance data for these energy systems are lacking and rarely reported.

The profitability of GSHPs in a life-cycle perspective has been considered previously by several authors. Rad, Fung, and Leong (2013), Hakkaki-Fard et al. (2015), Paiho, Pulakka, and Knuuti (2017), and Biglarian, Saidi, and Abbaspour (2019) have compared GSHPs and hybrid systems for detached single-family houses with other heating solutions using life-cycle costs. Compared to air-source heat pumps (ASHP), the profitability of a GSHPs is predicated on having a higher seasonal performance factor. Hakkaki-Fard et al. (2015) finds that the payback period of a GSHP is in excess of 15 years compared to an ASHP in Quebecois climate, while Paiho, Pulakka, and Knuuti (2017) and Biglarian, Saidi, and Abbaspour (2019) both find that a GSHP is cheaper than an ASHP over a period of 20 years in Finnish and Iranian climates, respectively. Contrary to the findings of Paiho, Pulakka, and Knuuti (2017) (Finnish climate), both Rad, Fung, and Leong (2013) (Canadian climate) and Biglarian, Saidi, and Abbaspour (2019) (Iranian climate) find that additional solar-thermal energy reduces the life-cycle costs of a GSHP system.

Similar life-cycle-cost studies have been used to optimize a solar-assisted GSHP system configuration (Weeratunge

Received February 17, 2022; accepted June 30, 2022
Vetle Kjær Risinggård, PhD, is a Researcher. **Ove Sivertsen**, is a the CEO of B. Fondenes AS. **Ulrik Thisted, PhD**, is a Senior Researcher. **Kirsti Midttømme, PhD**, is a Chief Scientist. None of the authors have an ASHRAE membership.
*Corresponding author e-mail: veri@norceresearch.no

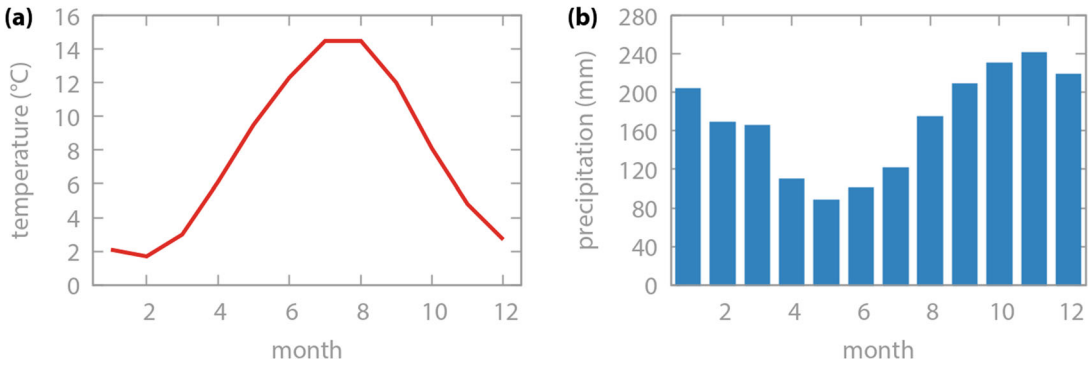

Fig. 1. Normal monthly temperatures and precipitation for Flesland Airport. (a) Normal monthly temperature. (b) Normal monthly precipitation. Climate data are reproduced from the Norwegian Meteorological Institute (2017) and are based on the most recent climate normal (1991–2020) (World Meteorological Organization 2017).

et al. 2018) as well as demand–response actions (Alimohammadisagvand et al. 2016).

Studies considering the life-cycle costs of GSHPs for larger buildings are less common. Paiho, Pulakka, and Knuuti (2017) considers a near zero-energy apartment building in addition to a detached house and finds that a conventional GSHP without solar assistance is cheaper in a life-cycle perspective than both an ASHP and district heating. Similar results are obtained by Marszal and Heiselberg (2011) in a Danish climate for a net zero-energy apartment building. Finally, Ristimäki et al. (2013) considers an entire district-heating system and finds that a system that derives its energy from GSHPs is more cost-efficient than one that derives its energy from excess heat from a thermal power station.

This study differs from previous studies in that it considers a commercial building rather than a residential building. Furthermore, the life-cycle cost is calculated using the measured energy performance of the case in question, rather than simulated values, as used by Marszal and Heiselberg (2011) and Paiho, Pulakka, and Knuuti (2017). The use of simulated values is a significant omission in the earlier literature, given that differences in energy performance are frequently reported between simulated and measured data (Kouhia, Nieminen, and Holopainen 2013; Pesola et al. 2016). With access to measured energy data, a detailed system description and performance study is also possible. To the best of our knowledge, this is the first published performance study of a GSHP system in Norway.

Reference case

The reference case considered in this paper is the Scandic Flesland Airport hotel, which is located at Flesland Airport outside Bergen, Norway (60.39°N, 5.32°E). The Bergen area has a mild coastal climate compared to the average Nordic climate. Normal monthly temperatures range between 1.7 °C (February) and 14.5 °C (July–August) and normal monthly precipitation ranges between 88.3 mm (May) and 240.7 mm (November), see Figure 1. The hotel was constructed in 2014–2017 and has a net floor area of 23,650 m^2 distributed over six floors (including the basement). It is intended to serve as a conference venue and has two conference halls with capacities of respectively 900 and 400 persons, in addition to 25 meeting rooms and 300 guest rooms. Figure 2 shows the hotel usage throughout the year. The number of guests is largest during the summer months (June–August).

The hotel's energy demand is dominated by heating due to the comparatively low outdoor temperatures (see Section "Performance study"). However, the power demand is dominated by cooling, with large cooling loads required over short periods to cool the conference halls. Space heating, domestic hot water, and cooling is provided by a BTES equipped with GSHPs. Additional domestic hot water is provided by solar thermal collectors. District heating is used to boost the water temperatures for space heating and domestic hot water and serves as a back-up. An adiabatic cooler serves as a back-up for peaks in the cooling loads. A simplified system schematic is provided in Figure 3.

The borehole thermal-energy storage (BTES) consists of a total of 50 vertical boreholes, each 200 m deep, drilled in granite and monzonite. The boreholes are connected in parallel in three sections of 17, 17, and 16 boreholes, respectively. The three sections are subsequently connected in parallel to each other. Double U-type (4 × 32 mm) turbo collectors are used. Turbo collectors have ribs in the inside, enabling turbulent flow at lower flow rates. Key features of the BTES are summarized in Table 1 and Figure 4.

The BTES is connected to four GSHPs with a total nominal capacity of 320 kW. Each heat pump has two scroll compressors, giving two steps per heat pump and a total of eight steps for the system.

Hot water for space heating and domestic hot water is heated to 50 °C by the heat pumps and accumulated in twelve 400-L accumulator tanks. These tanks also receive hot water from 60 m^2 of vacuum solar collectors, although the latter contribute less than 6% of the total energy for domestic hot water. The hot-water temperature is subsequently boosted to 70 °C using district heating in four separate 400-L tanks. Key features of the solar-thermal collectors are summarized in Table 2.

Cooling is distributed using the ventilation system. Heat is extracted from the ventilation air using heat exchangers and transferred to the BTES circulating fluid. The cold air is returned to the building, whereas the heated circulating fluid

is returned to the boreholes. While in transit through the borehole heat exchangers, the circulating fluid is returned to its original temperature by transferring the heat to the bedrock. This is referred to as *free cooling* below. A maximum of 380 kW of cooling power can be delivered using two 7.5 kW circulation pumps. An additional 220 kW of cooling can be delivered using an adiabatic cooler.

Performance study

The system performance data have been collected for the period January 2017–December 2020. Energy has been measured using Multical 602 energy meters from Kamstrup (Kamstrup A/S 2019) equipped with Ultraflow 54 DN15-125 flow meters (Kamstrup A/S 2022) and Pt500 EN 60 751 temperature sensors (Kamstrup A/S 2021). The energy meters are certified according to EN 1434 class C, and have a measurement uncertainty of <6%.

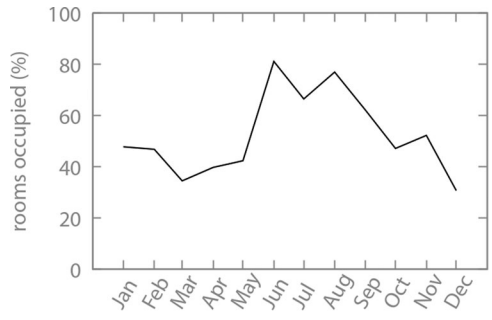

Fig. 2. Percentage of rooms occupied in 2018. Monthly averages.

Figure 5 shows the delivered energy throughout this period, as well as the heating seasonal performance factor (SPF) for the first two years. The SPF is calculated as

$$\mathrm{SPF} = \frac{Q_{\mathrm{SH}} + Q_{\mathrm{DHW}}}{W}, \tag{1}$$

where Q_{SH} is the energy delivered as space heating, Q_{DHW} is the energy delivered as domestic hot water, and W is the electricity supplied to the GSHP and the circulation pumps. The energy extracted from and injected into the BTES is shown in Figure 6 together with the thermal balance ratio (ratio of extracted to injected heat).

The hotel was opened April 4, 2017, but the heat pumps started running in November 2016. Still, Figures 5 and 6 show clear differences between 2017 and the subsequent years. More heat was extracted from the BTES in 2017, and less heat injected. Consequently, the thermal balance ratio for 2017 is 24.4, in contrast with 8.3 in 2018. The SPF is also lower in 2017 (4.2) than in 2018 (4.5). 2018 and 2019 were both normal years of operation, and the datasets for the two years are similar. Due to Covid-19 travel restrictions, the hotel closed in February 2020, and was only partly reopened later that year. As a result, the heating loads in particular were considerably smaller in 2020 than in the preceding years.

Figures 5 and 6 demonstrate that the energy demand of the building is dominated by heating. The data for 2018 through 2020 broken down into monthly values is shown in

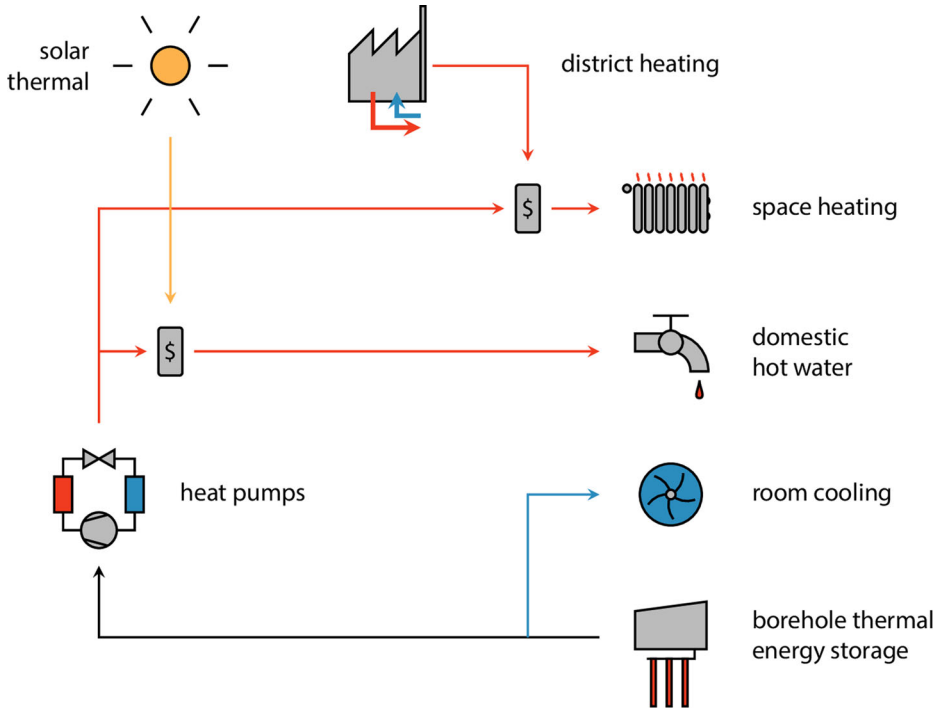

Fig. 3. Simplified schematic of the energy system of the Scandic Flesland Airport hotel. Heat is extracted from the BTES by a heat pump for space heating and domestic hot water and injected into the boreholes for cooling. District heating boosts the hot-water temperature and serves as a back-up. Additional hot water is provided by solar thermal collectors.

Table 1. Summary of borehole thermal-energy storage key features.

feature	value
ground source	vertical boreholes
ground composition	granite, monzonite
ground temperature (undisturbed)	8.8 °C
ground thermal conductivity	5.0 W/m·K (estimated from thermal response test)
ground heat capacity	850 J/kg·K
groundwater level	3 m below borehole cap
number of boreholes	50
borehole length	200 m
borehole diameter	115 mm
borehole filling material	only groundwater
borehole heat exchanger	double U-tube ($d = 32$mm)
borehole thermal resistance	0.105 m·K/W (heating) 0.085 m·K/W (cooling)
loop type	closed loop
circulating fluid	75% water and 25% Dowcal 200 (propylene glycol)

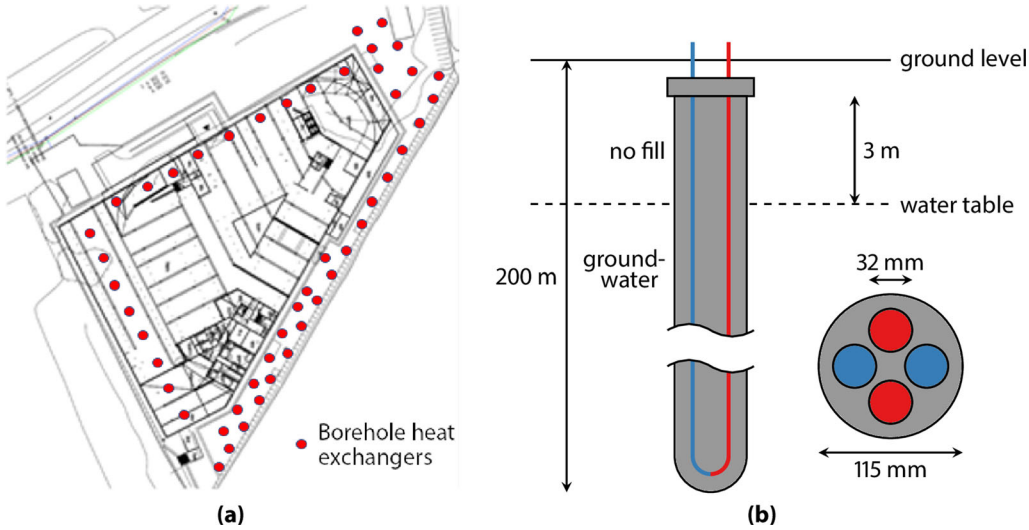

Fig. 4. (a) Borehole distribution relative to the Scandic Flesland Airport hotel. (b) Borehole and borehole heat exchanger design.

Table 2. Summary of solar-thermal collector key features.

feature	value
collector type	vacuum
orientation	South
angle with vertical	45°
number of panels	25
panel area	2.4 m^2
net area	60 m^2
loop type	closed loop
circulating fluid	water

Figure 7. Space heating dominates during the winters, whereas the cooling loads reach values comparable to the heating loads during the summer months. The reduction in the heating loads during the summer is entirely due to a reduction of space heating—domestic hot-water loads actually show a small increase. This is consistent with the larger number of guests at the hotel in this period (Figure 2). The absence in Figure 7 of significant hot-water loads in 2019 is due to gaps in the dataset. However, the unusually small loads in March and April in 2020 are due to the hotel being closed because of Covid-19 travel restrictions.

Monthly loads for 2018 are shown in Figure 8 together with the heating monthly performance factor. The 2018 SPF is 4.5, however monthly performance factors reach 5.0 in May and July. This is due to the high temperatures of the circulating fluid extracted from the boreholes and the high outdoor temperatures in these months. Monthly average entering and exiting temperatures from the BTES as well as the outdoor monthly average temperature for 2018 are plotted in Figure 9a.

Because heat is predominantly being extracted in the winter and injected during the summer, the borehole temperatures in Figure 9a go through a seasonal cycle that is similar to the outdoor temperatures. The yearly average temperatures of the extracted circulating fluid have fallen in the

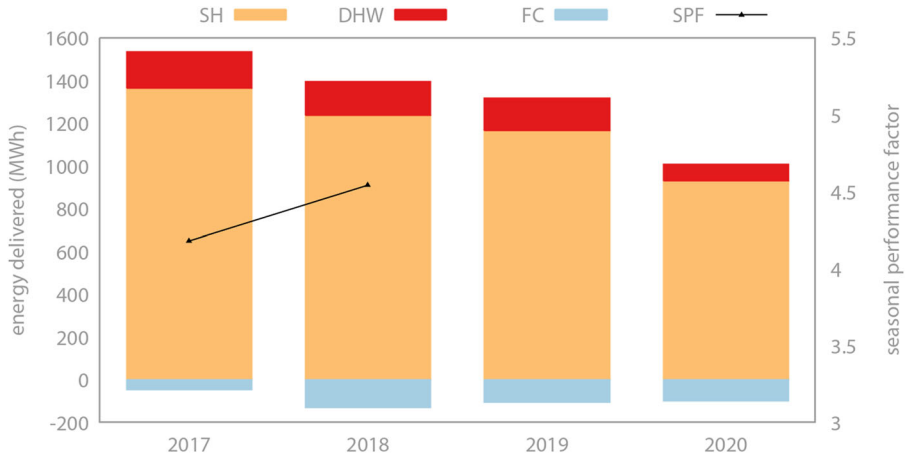

Fig. 5. Energy delivered by the GSHPs and free cooling using the BTESs in 2017–2020, and the SPF. The abbreviations in the legends translate to, respectively, space heating (SH), domestic hot water (DHW), free cooling (FC), and heating seasonal performance factor (SPF).

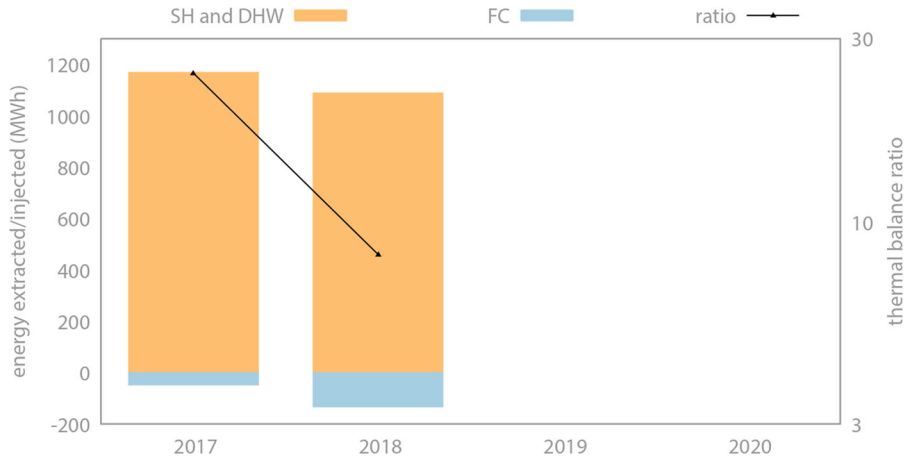

Fig. 6. Energy extracted from and injected into the BTES in 2017–2020. The abbreviations in the legends translate to, respectively, space heating (SH), domestic hot water (DHW), and free cooling (FC). Ratio is short for thermal balance ratio (ratio of extracted to injected heat).

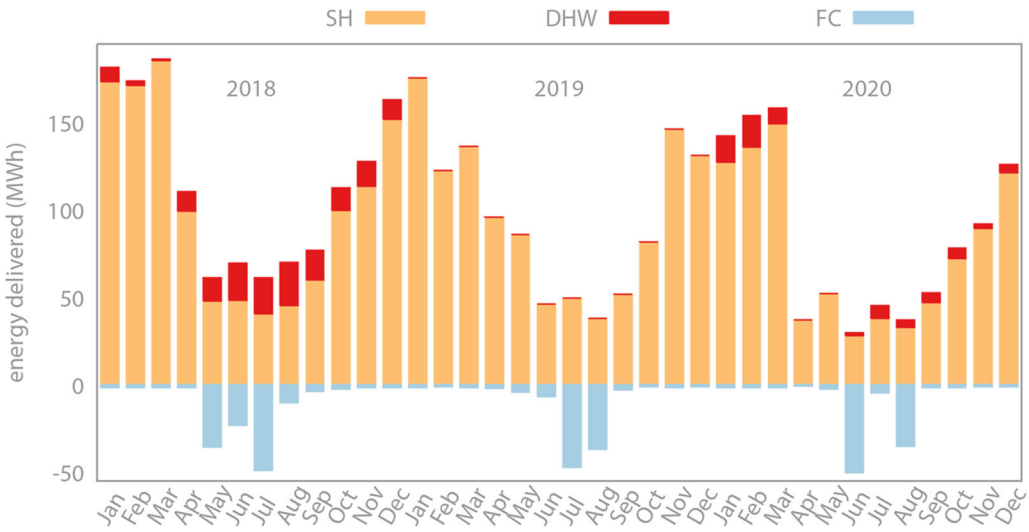

Fig. 7. Monthly energy delivered by the GSHPs and free cooling using the BTES in 2018–2020. The abbreviations in the legends translate to, respectively, space heating (SH), domestic hot water (DHW), and free cooling (FC).

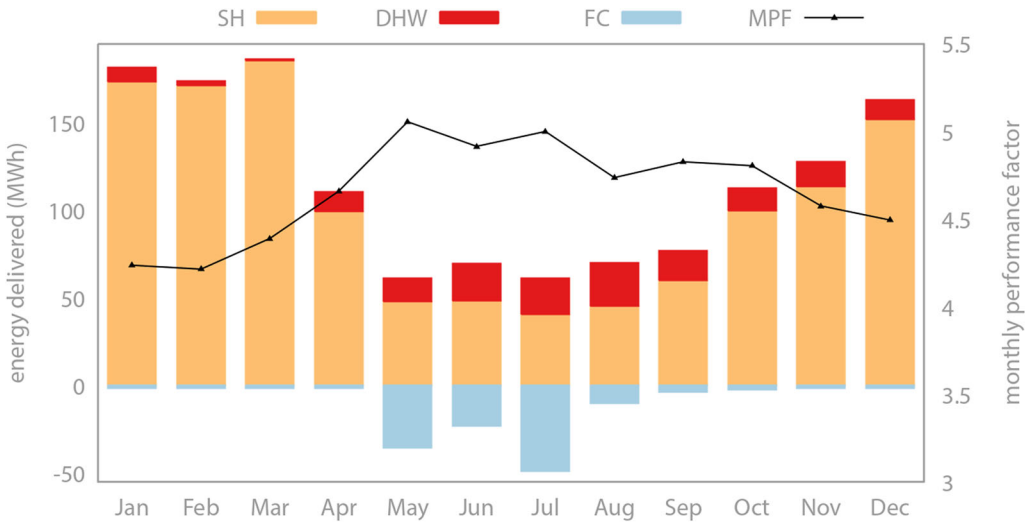

Fig. 8. Monthly energy delivered by the ground-source heat pumps and free cooling using the borehole heat exchangers in 2018 and the monthly performance factor. The abbreviations in the legends translate to, respectively, space heating (SH), domestic hot water (DHW), free cooling (FC), and heating monthly performance factor (MPF).

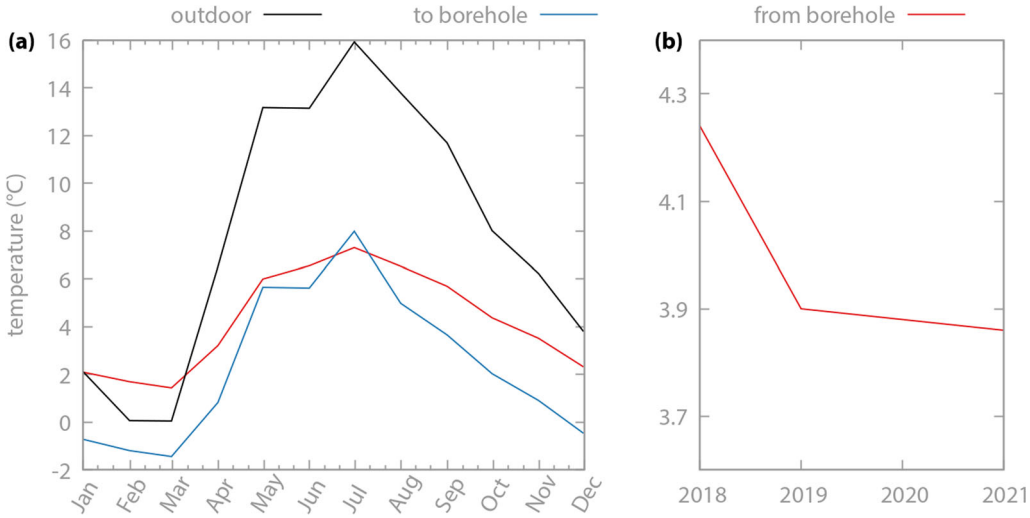

Fig. 9. (a) Monthly average entering and exiting temperatures from the BTES for 2018. The monthly average outdoor temperature is also plotted. (b) Yearly average exiting temperatures from the BTES for 2018–2021.

period 2018–2021, but may be stabilizing as shown in Figure 9b. A possible explanation might be that the BTES is reaching a steady state in which the temperature difference between the BTES and the surrounding rock matches the heat flux necessary for supplying the net amount of heat extracted yearly. A significant groundwater flux observed in some of the boreholes might also be a contributing factor. However, the limited amount of time since operations began prevents firm conclusions from being drawn yet.

The daily average circulating fluid temperatures are plotted against the outdoor daily average temperature in Figure 10. The crossing point in Figure 10 at approximately 15 °C indicate that at this temperature the building's energy demand changes from heating-dominated to cooling-dominated. A similar crossing point is seen in the building's energy signature in Figure 11. It is the fact that the yearly normal temperature is less than 15 °C (Figure 1) that gives rise to the overall heating-dominated energy demand. The comparatively small number of days with outdoor daily average temperatures above 15 °C is reflected in the comparatively small number of scatter points above 15 °C in Figures 10 and 11. The overall heating-dominated energy demand is more clearly shown in the heating- and cooling-load duration curves for 2018 shown in Figure 12. In 2018, the energy demand for cooling was only 9% of the energy demand for heating.

The highest measured heating power of 2018 was approximately 350 kW, a value that agrees well with the heating duration-curve maximum of 7.5 MWh/day. Similarly, the highest measured free-cooling power of 2018 of approximately 380 kW, agrees well with the cooling duration-curve maximum of 8 MWh/day. However, the maximum total cooling power was approximately 600 kW, fully utilizing

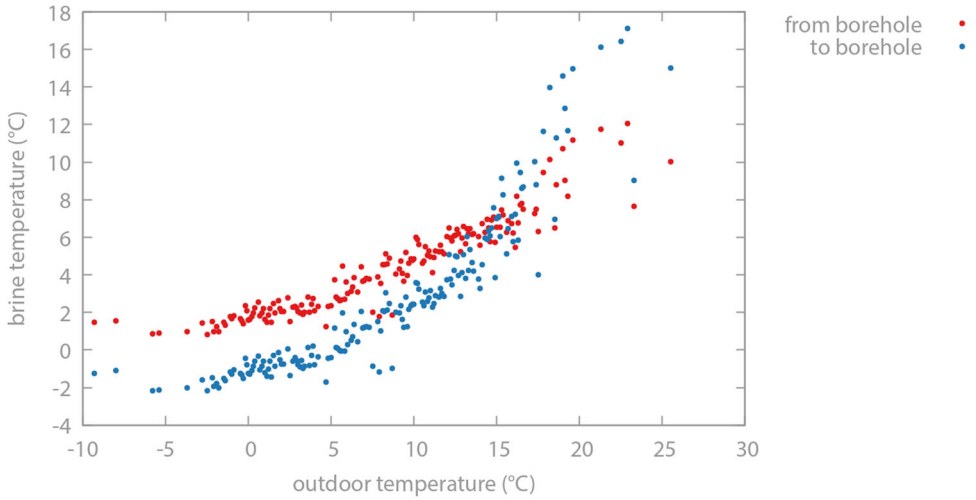

Fig. 10. Daily average entering and exiting temperatures from the BTES for 2018 versus the outdoor daily average temperature.

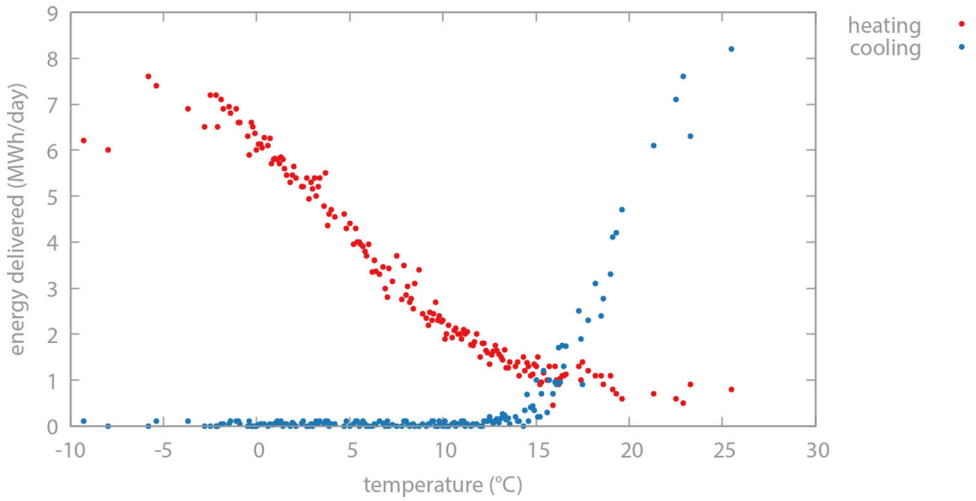

Fig. 11. Daily space-heating and free-cooling loads for 2018 versus the outdoor daily average temperature.

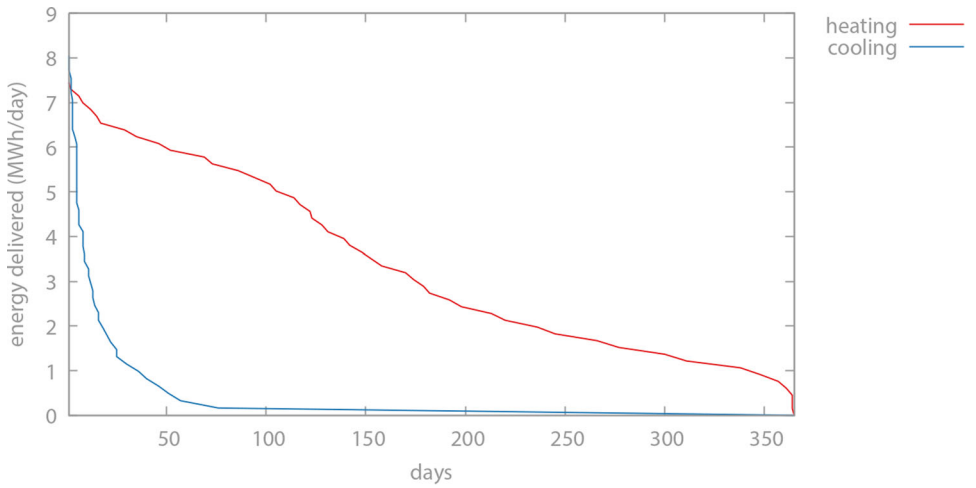

Fig. 12. Duration curve for 2018 based on daily values for space heating and free cooling.

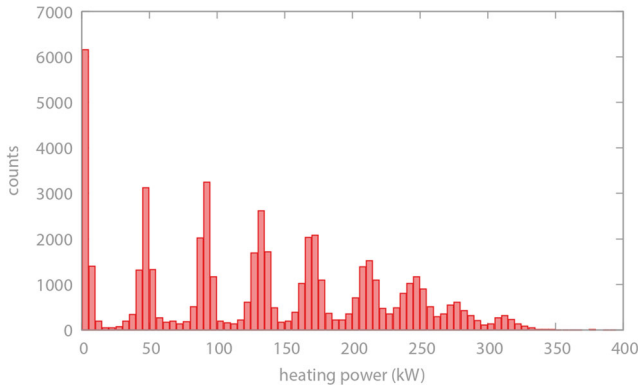

Fig. 13. Histogram of measured heating power in 2019 based on values recorded every 10 minutes.

both the free cooling and the adiabatic cooling. Comparing peak heating (350 kW) and cooling (600 kW) power, it is clear that although the energy demand of the building is dominated by heating, its power demand is dominated by cooling by a factor of 1.7.

Prior to construction, the desired number of boreholes was determined based on the cooling power that was required to be met by free cooling (380 kW). The relative size of the heat pumps and the BTES is a result of the heat-pump capacity being determined independently based on the required heating power to be met by the system. The solar thermal collectors cover only 6% of the domestic hot-water heating loads.

A histogram of the measured heating power in 2019 is shown in Figure 13. The eight steps of the GSHP are clearly recognizable. Summing the recorded counts for all eight steps and comparing with the number of counts in the off state shows that the GSHP was in operation 85% of the time in 2019. The GSHP on and off times and step selection is chosen automatically based on a hot-water temperature set-point that depends on the outdoor temperature, as well as the indoor temperature throughout the building. A similar operation strategy is used for the circulation pumps that deliver circulating fluid to the air–fluid heat exchanger that cools the ventilation air.

Alternative cases

To assess the economic advantages and disadvantages of the chosen heating and cooling solutions, two alternative cases were defined. In the following, the reference case will be referred to as Alternative 1, and the two alternative cases as Alternatives 2 and 3.

Alternative 2 represents a "default" energy system for similar buildings in areas where district heating is available. It employs a standard heating solution based on district heating. Compared to Alternative 1, this eliminates the need for the BTES, the GSHPs, and the associated equipment. In the absence of the GSHP system, free cooling and the adiabatic cooler are substituted with a dry-cooler system of equivalent capacity. A revised schematic of the energy system is shown in Figure 14.

Alternative 3 represents a default energy system for similar buildings outside district-heating licensing areas. It employs a standard heating solution based on electricity. Compared to Alternative 1, this removes the need for the BTES, the GSHPs and the associated equipment, and the district-heating installations. Similarly to Alternative 2, the free cooling and the adiabatic cooler are substituted with a dry-cooler system of equivalent capacity. A revised schematic of the energy system is shown in Figure 15.

Alternatives 1–3 all include 60 m^2 of solar thermal collectors that provide domestic hot water. In 2018, the solar collectors covered only 6% of the total domestic hot-water energy consumption for the reference case (Alternative 1). For each of Alternatives 1 through 3, life-cycle cost analyses have therefore been carried out both including and excluding solar collectors.

Life-cycle cost analysis: Framework

The present life-cycle cost analysis is limited to the heating and cooling system of the building. Cost items that are common to all alternatives, such as radiators for space heating and ventilation ducts for cooling, have been neglected.

The heating and cooling system takes up physical space in the building and contributes a fraction of its electricity consumption. Costs related to the structural components of the building have therefore been assigned to each alternative based on the area they occupy. Similarly, each alternative has been assigned a fraction of the costs of the electricity-supply infrastructure based on the fraction of the total electricity consumption it contributes.

Cost data was collected from the original building plans, as well as from publicly available material in the published literature and government reports. By cross-checking costs from the original plans against published national averages and making adjustments where necessary, a cost level representative of a generic building similar to the original hotel was ensured. References for published costs are presented in Table 3.

All costs are reported in 2020 Norwegian kroner (NOK). Costs from the original building plans and older published values have been converted to 2020 values using the consumer price index of Statistics Norway (Statistics Norway 2021b),

$$c(t_0) = c(t') \cdot \frac{I(t_0)}{I(t')}. \tag{2}$$

Here, t_0 denotes year 2020, t' denotes the date of the cost data, $c(t)$ is the cost at time t, and $I(t)$ is the consumer price index at time t. Values in 2020 Norwegian kroner can be converted to values in 2020 US dollars (USD) using the average 2020 exchange rate of 9.34 NOK/USD. Future maintenance and replacement costs, energy costs, and decommissioning costs have been discounted to the present using an interest rate of 4% for the first 39 years of operation, and 3% for subsequent years as recommended by the Norwegian Ministry of Finance (2021). Given a future value

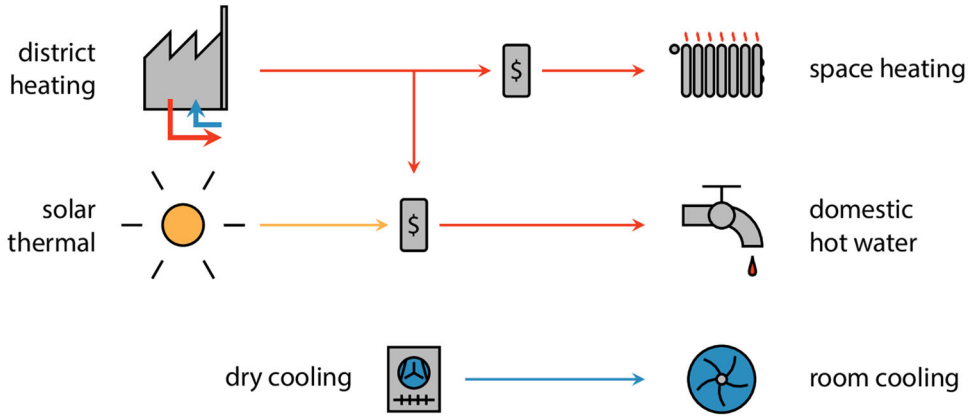

Fig. 14. Simplified schematic of a "default" energy system for buildings in areas where district heating is available (Alternative 2). District heating provides space heating and domestic hot water. Additional hot water is provided by solar thermal collectors. Cooling is provided by dry cooling.

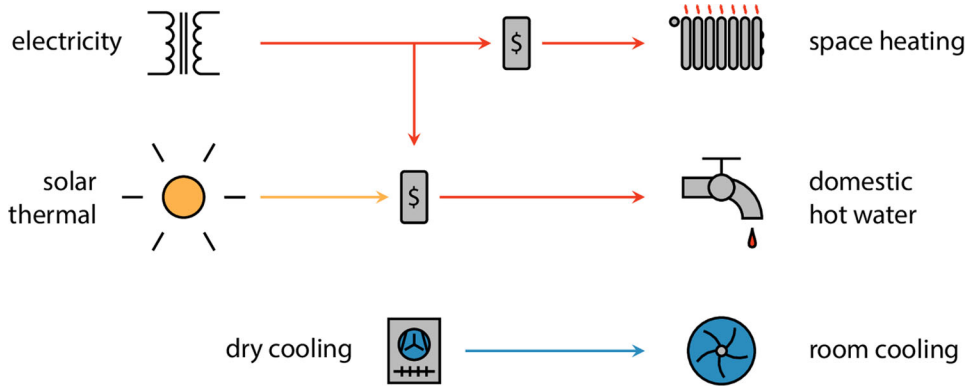

Fig. 15. Simplified schematic of a "default" energy system for buildings outside district-heating licensing areas (Alternative 3). Space heating and domestic hot water is provided using electricity. Additional hot water is provided by solar thermal collectors. Cooling is provided by dry cooling.

Table 3. References for published costs.

Topic	References
borehole thermal-energy storage	Traaen (2018)
ground-source heat pumps	Sidelnikova et al. (2015)
solar thermal collectors	Sidelnikova et al. (2015) and Rindal and Salvesen (2008)
district heating	Sidelnikova et al. (2015)
electricity supply infrastructure	Uthus, Samdal, and Trengereid (1998)
projected electricity costs	Birkelund et al. (2021)
adiabatic cooler	Strand-Hansen and Bugge (2020)
building construction, maint., and holding costs	Norconsult Informasjonssystemer AS and Bygganalyse AS (2021)

c_n at n years into the future and an interest rate r, the present value c_0 is calculated as (Wijst 2013)

$$c_0 = \frac{c_n}{(1+r)^n}. \tag{3}$$

The building lifetime has been set to 50 years.

Uncertainties have been estimated for all cost elements. The method of estimation depends on the cost element in question, but falls broadly into one of four categories:

1. Negligible uncertainty. Example: Floorspace costs for Alternative 1.
2. Uncertainty determined by measurement uncertainty. Example: Temperature, flow, and power measured using Kamstrup energy meters.
3. Reported uncertainty for published data. Example: Future electricity costs taken from (Birkelund et al. 2021).
4. Uncertainty estimated by competent professionals. Example: Cost of the dry-cooling solutions for Alternatives 2 and 3.

The net uncertainty for the total cost has been calculated from the individual uncertainties using the Gaussian law of error propagation (Taylor 1997),

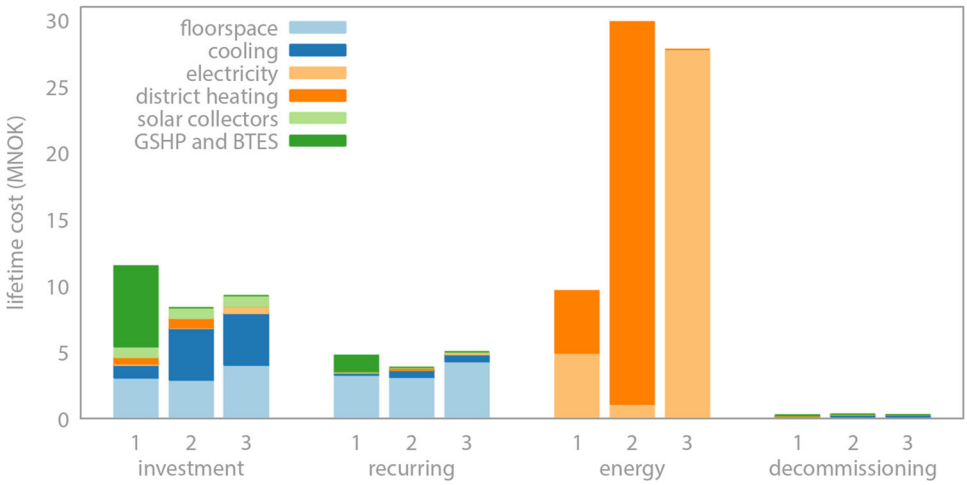

Fig. 16. Summary of life-cycle costs for Alternatives 1–3 with solar collectors broken down by cost category and cost drivers. Costs for each alternative within each cost category are represented as stacked bars. Recurring costs have been divided into energy costs and other recurring costs. All costs are given in millions of NOK (MNOK). 1 MNOK equals 0.11 million USD.

$$\delta f = \sqrt{\left(\frac{\partial f}{\partial x}\delta x\right)^2 + \left(\frac{\partial f}{\partial y}\delta y\right)^2 + \cdots}, \tag{4}$$

where f is the derived quantity (life-cycle cost), x and y are quantities of known uncertainty (cost elements), and δx, δy and δf are the uncertainties. For sums, this formula simplifies to

$$\delta f = \sqrt{(\delta x)^2 + (\delta y)^2 + \cdots} \tag{5}$$

as $\partial f/\partial x = \partial f/\partial y = \cdots = 1$.

The most important contribution to the net uncertainty arises from year-to-year variations in the weather and the number of guests, and enters the life-cycle-cost calculation through the energy data. The energy data are based on 2018 values. As pointed out in Section "Performance study", 2018 was a normal year of operation for the hotel.

Meteorological data indicate that the yearly average temperature of 2018 was 1.2 °C above the yearly normal value and the yearly precipitation was 1.03 times larger than the normal value (Grinde et al. 2019). However, the winter months February and March were colder than normal (Grinde et al. 2019), and the summer of 2018 was unusually dry and warm (Skaland et al. 2019). This contributed to the larger heating as well as cooling loads of 2018 compared to 2019 (Figure 5). As a result, using energy data for 2018 in the life-cycle cost analysis might overestimate the energy costs of the reference case. However, the 2018 energy data are still representative for a mild coastal climate in the Nordic region and comparable locations worldwide.

The yearly average temperature at Flesland has a standard deviation of 0.7 °C calculated over the period of the most recent climate normal (1991–2020). Combined with the building's energy signature in Figure 11, this gives an expected yearly variation of about 8% in the energy consumption. Taking into account the variation in the number of guests as well, the overall uncertainty of the energy consumption is estimated to 20%.

Life-cycle cost analysis: Results

Figure 16 summarizes the life-cycle costs of Alternatives 1 through 3 with solar collectors broken down by cost categories and cost drivers. These costs are also given in Table 4 The same costs—except the energy costs—are shown in separate charts in Figure 17, including uncertainty estimates. The stacked bars in Figure 16 facilitate comparison of costs *across* cost categories, whereas Figure 17 facilitates comparisons of costs as well as uncertainties *within* cost categories.

The investment of the BTES and GSHPs dominates the initial costs incurred by Alternative 1 (Figure 17a). The second-largest cost driver is the floorspace, or the portion of the cost of the structural components of the building assigned to the heating and cooling system. As seen in Figure 16, the initial floorspace cost is larger for Alternative 1 than for Alternative 2 because of the area occupied by the heat pumps, the circulation pumps, and the other equipment associated with the ground-source system. The floorspace cost is in turn larger for Alternative 3 than for Alternatives 1 and 2 because the all-electric Alternative 3 has to carry a larger fraction of the floorspace cost of the electricity infrastructure. Figure 17 also shows that for Alternatives 2 and 3, the initial cost of the dry coolers and refrigeration machines roughly equals the floorspace cost.

Recurring costs have been divided into energy costs and other recurring costs, namely maintenance and replacement of equipment that reaches end-of-life. The other recurring costs are dominated by the floorspace costs. When comparing the floorspace costs to the other recurring-cost drivers in Figure 17, it is important to take into account that only 34% of the recurring floorspace costs are due to maintenance—the remaining floorspace costs account for building taxes, insurance, administration, and periodic upgrade costs. The relative size of the floorspace costs is the same for the initial investment and the recurring costs. Conversely, Figure 16 shows that the ratios of maintenance costs of the energy system itself change significantly going from the initial to the

Table 4. Summary of life-cycle costs for Alternatives 1–3 with solar collectors broken down by cost category and cost drivers. Recurring costs have been divided into energy costs and other recurring costs. All costs are given in thousands of NOK (kNOK). 1 kNOK equals 110 USD.

description	investment	recurring	energy	decom.
Alternative 1				
GSHP and BTES	6,071	1,227		58
solar collectors	800	43		11
district heating	511	40	4,657	62
electricity	68	1	4,947	2
cooling	989	183		34
floorspace	3,048	3,258		104
Alternative 2				
GSHP and BTES	0	0		0
solar collectors	800	43		11
district heating	691	160	28,792	62
electricity	20	0	1,096	1
cooling	3,910	530		148
floorspace	2,906	3,106		107
Alternative 3				
GSHP and BTES	0	0		0
solar collectors	800	43		11
district heating	0	0	0	0
electricity	531	165	27,796	7
cooling	3,910	530		148
floorspace	4,006	4,282		107

recurring costs. This can be seen most clearly when comparing the total initial and recurring costs of Alternatives 1 and 3: Due to the low maintenance costs of the ground-source system, the recurring costs of Alternatives 1 and 3 are approximately equal, whereas the initial investment is significantly larger for Alternative 1.

As seen in Figure 16, the energy costs are the largest cost category and is the decisive factor when comparing the total life-cycle costs of Alternative 1 with those of Alternatives 2 and 3. Overall, Alternative 1 is significantly cheaper than Alternatives 2 and 3 due to the large amount of free energy that can be extracted from the ground. Still, the electricity costs of Alternative 1 are larger than those of Alternative 2 because the amount of electric energy required for running the GSHPs is larger than the one required for running the dry coolers and refrigeration machines. At the same time, the overall energy cost of Alternative 3 is smaller than that of Alternative 2, despite the district-heating energy price being identical to the electricity price, because the electricity grid tariff is smaller than the equivalent tariff for district heating.

The results in Figures 16 and 17 include solar thermal collectors for all three alternatives. As seen in Figure 17, the initial investment of the solar thermal collectors is 800 kNOK. Adding recurring costs of 43 kNOK and decommissioning costs of 11 kNOK, the total life-cycle cost of the solar thermal collectors is 854 kNOK. Based on 2018 values the solar thermal collectors are assumed to deliver 24.3 MWh of energy to domestic hot water yearly. In the absence of solar thermal collectors, this energy would be covered using district heating for Alternatives 1 and 2, or electricity for Alternative 3, costing respectively 420 kNOK and 390 kNOK. Comparing these numbers with the life-cycle cost of the solar thermal collectors, it is evident that the solar thermal collectors operate at a loss over the building lifetime for all three alternatives. However, the contribution from the solar thermal collectors to the total life-cycle cost is relatively small, and Alternative 1 is still significantly less costly than Alternatives 2 and 3, even if the solar thermal collectors are removed for the latter cases.

Figures 18 and 19 show the sensitivity of the life-cycle costs on the energy price and the space-heat consumption. Considering first the energy price, the same energy price has been used for both electricity and district heating, following a common policy among Norwegian district-heating providers (Norwegian Ministry of Petroleum and Energy 1990). Norwegian energy prices are expected to stay in the range 350–650 NOK/MWh over the next 20 years (Birkelund et al. 2021) and not exceed European prices (shaded area in Figure 18). Interestingly, Figure 18 shows that Alternative 1 will remain cheaper than Alternatives 2 and 3 even if energy prices approach zero, provided that usage-dependent grid tariffs and taxes remain at current levels. As expected, Alternative 1 becomes more profitable with respect to Alternatives 2 and 3 as the energy price increases, implying that GSHPs are an even better investment for a building of this type in locations with higher energy prices.

Considering the sensitivity of the results to space-heat consumption enables an assessment of the validity of these results in locations with climates that are different from that of the reference location. Figure 19 shows the total life-cycle cost as a function of space-heat consumption spanning a range of 0.5–1.5 times the consumption of the reference case. A crossing point is expected at about zero space heating, assuming constant domestic hot-water demand. The profitability of Alternative 1 with respect to Alternatives 2 and 3 over this entire range indicates that GSHPs represent a profitable investment not only in the Nordics, but throughout much of Europe. The European Union average space-heat consumption (kWh/m^2) is in fact larger than the space-heat consumption of both Sweden and Denmark (Bertelsen and Vad Mathiesen 2020)—both of which are locations with climates and building standards comparable to the reference case.

The above discussion neglects the dependence of cooling costs on climatic conditions. Increased cooling loads are expected to have a twofold effect: First, for the borehole temperatures considered in the reference case, the cost of cooling is larger for Alternatives 2 and 3 than for Alternative 1. Second, borehole temperatures will rise as the thermal balance ratio decreases with increasing cooling loads, thus improving the SPF. Thus, increased cooling loads favor Alternative 1 over Alternatives 2 and 3. On the other hand, decreased cooling loads are expected to have a limited effect as the energy demand for cooling is currently only 9% of the energy demand for heating.

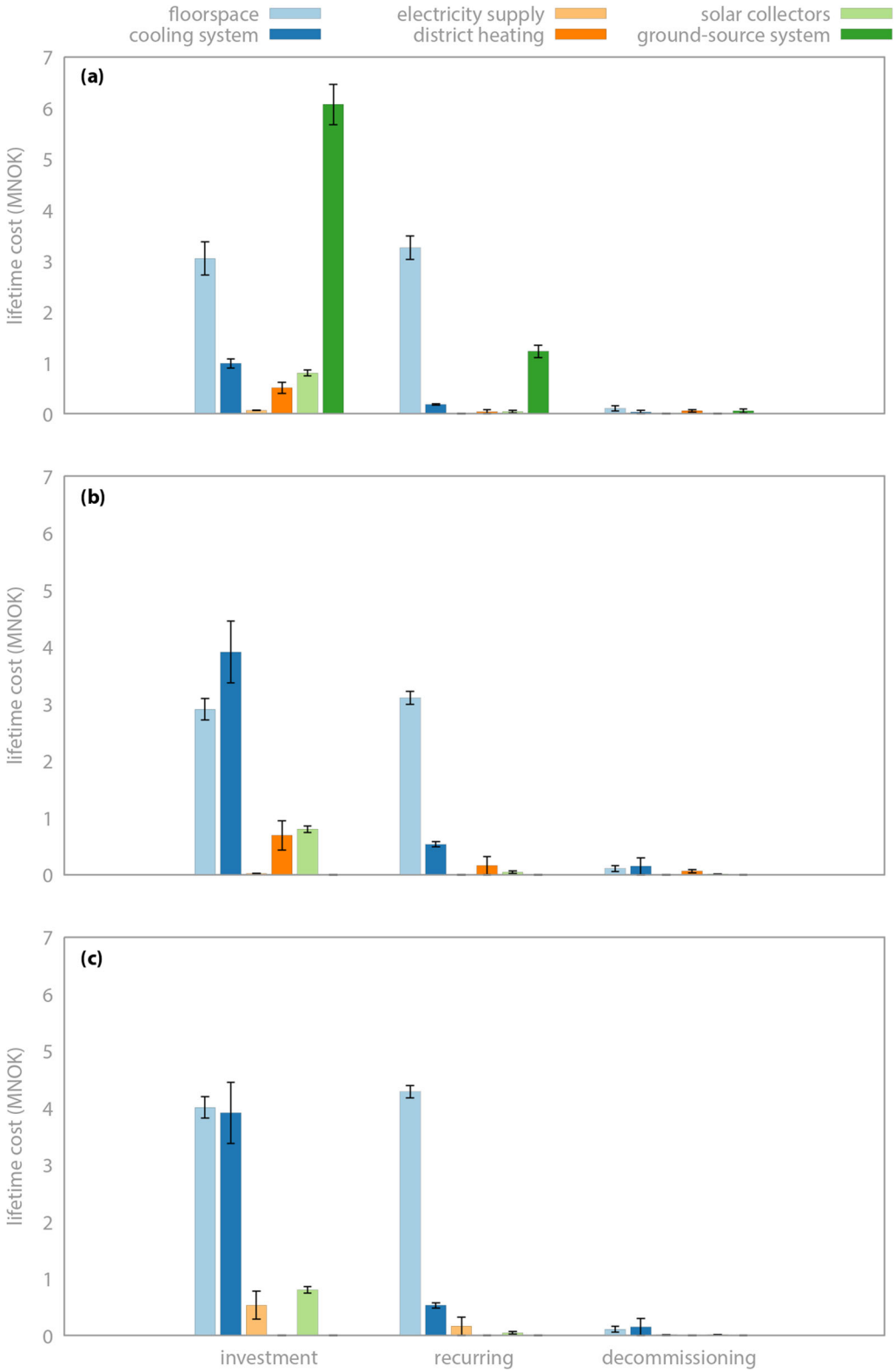

Fig. 17. Summary of life-cycle costs for (a) Alternative 1, (b) Alternative 2, and (c) Alternative 3. All alternatives are broken down by cost category and cost drivers and include solar collectors. All costs are given in millions of NOK (MNOK); 1 MNOK equals 0.11 million USD.

Comparing the present values of different options—represented here by the life-cycle costs of the three alternatives—is a powerful tool to guide investments. However, other key numbers are also often used to measure investment performance. In particular, the internal rate of return of a project is often used as guide because of the ease with which

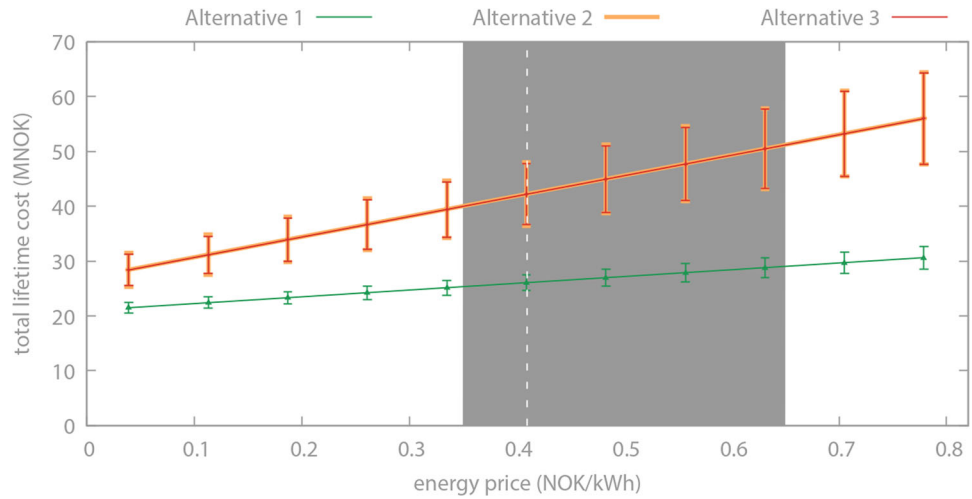

Fig. 18. Sensitivity of total life-cycle cost for Alternatives 1–3 with solar collectors to the energy price (excluding usage-dependent grid tariffs and taxes). The shaded area indicates the expected range of Norwegian energy prices over the next 20 years, and the dashed white line indicates the energy price used for Figures 16 and 17 and Table 4. Costs are given in millions of NOK (MNOK). 1 MNOK equals 0.11 million USD.

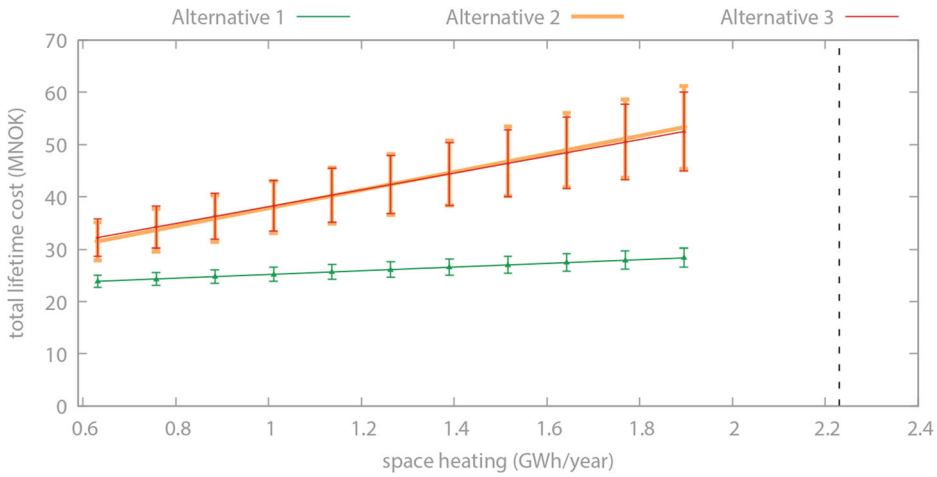

Fig. 19. Sensitivity of total life-cycle cost for Alternatives 1–3 with solar collectors to the space-heat consumption. The dashed line indicates the space-heat consumption of the hotel that would be expected given an EU-average space-heat consumption of 113 kWh/m^2. Costs are given in millions of NOK (MNOK). 1 MNOK equals 0.11 million USD.

this number can be compared to other investments. The internal rate of return is the interest rate r for which the project has a net present value of zero (Wijst 2013),

$$\sum_{n=0}^{m} \frac{c_n}{(1+r)^n} = 0. \tag{6}$$

Here, c_n is the is the cost of or return on the project in year n, and m is the project lifetime in years.

Although all of the three alternatives represent a net cost, an internal rate of return can still be calculated for choosing Alternative 1 over Alternative 2 or 3—with positive cash flows coming from the yearly energy-bill savings due to extraction of free energy from the ground. To obtain annual discounted cash flows, present values of the recurring costs have been converted to equivalent annual costs by dividing by appropriate annuity factors (Wijst 2013),

$$c_e = \frac{rc_0}{1-(1+r)^{-m}}, \tag{7}$$

where c_e is the equivalent annual cost, c_0 is the present value of the recurring costs, r is the interest rate, and m is the project lifetime in years. Table 5 shows the yearly cash flows for two scenarios: choosing Alternative 1 over Alternative 2 and choosing Alternative 1 over Alternative 3. The negative cash flows in year 1 and 50 represent investments and decommissioning costs incurred by Alternative 1. The positive cash flows in years 2–49 represent the alternative energy costs saved by choosing Alternative 1 over Alternative 2 or 3, minus the maintenance costs of Alternative 1. The internal rate of return of the net cash flows in the first line of Table 5 (choosing Alternative 1 over Alternative 2) is 5.9%. The internal rate of return of

Table 5. Cash flows for calculation of internal rates of return.

Option	1	2–49	50	IRR
Alt. 1 vs. 2	−11,486	+723	−272	5.9%
Alt. 1 vs. 3	−11,486	+626	−272	4.9%

the net cash flows in the second line of Table 5 (choosing Alternative 1 over Alternative 3) is 4.9%. GSHPs thus represent a more profitable investment in district-heating licensing areas (mandatory use of district heating), because the electricity grid tariff—and thus the energy bill—is smaller than the equivalent tariff for district heating.

Conclusion

To conclude, a performance study has been carried out for the ground-source heating and cooling system of the hotel Scandic Flesland Airport located in Bergen, Norway. The building has a heating-dominated energy demand, cooling only being necessary for outdoor daily average temperatures in excess of 15 °C. However, the building's power demand is cooling dominated on account of brief surges in cooling power during daytime hours in the summer. This was accounted for in the construction phase, and explains the relative size of the GSHPs and the BTES. The heating system operates at a SPF of 4.5 in normal years, with monthly performance factors reaching 5.0.

A life-cycle cost analysis has been carried out for the as-build reference case and two alternative cases representing default systems respectively inside and outside district-heating licensing areas. The life-cycle costs for the as-built system are considerably less than the alternatives due to the free energy that can be extracted from the ground. Yet, the solar thermal collectors are not a profitable addition to the energy system due to their high cost and low production of hot water.

Sensitivity analyses with respect to energy prices and space-heat consumption demonstrate that the results are robust and have an area of validity extending over much of Europe and comparable locations worldwide. The internal rate of return on choosing the as-built solution over district heating and electric heating is 5.9% and 4.9%, respectively.

Funding

This work was supported by Norges Forskningsråd, grant number 281000; Enova SF, grant number 18/3576.

ORCID

Vetle Kjær Risinggård http://orcid.org/0000-0002-4841-6027

References

Alimohammadisagvand, B., J. Jokisalo, S. Kilpeläinen, M. Ali, and K. Sirén. 2016. Cost-optimal thermal energy storage system for a residential building with heat pump heating and demand response control. *Applied Energy* 174 (July):275–87. doi:f8rrx7. doi:10.1016/j.apenergy.2016.04.013

Bertelsen, N., and B. Vad Mathiesen. 2020. EU-28 residential heat supply and consumption: Historical development and status. *Energies* 13 (8):1894. doi:gm4vb8. doi:10.3390/en13081894

Biglarian, H., M. H. Saidi, and M. Abbaspour. 2019. Economic and environmental assessment of a solar-assisted ground-source heat pump system in a heating-dominated climate. *International Journal of Environmental Science and Technology* 16 (7):3091–8. doi:gmh44s. doi:10.1007/s13762-018-1673-3

Birkelund, H., F. Arnesen, J. Hole, D. Spilde, S. Jelsness, F. H. Aulie, and I. E. Haukeli. 2021. *Langsiktig kraftmarkedsanalyse 2021–2040 [Long-term electricity market analysis: 2021–2040]. 29-2021*. Oslo, Norway: Norwegian Water Resources and Energy Directorate.

Cozzi, L., T. Gül, S. Bouckaert, A. F. Pales, C. McGlade, U. Remme, B. Wanner, et al. 2021. *Net zero by 2050. A roadmap for the global energy sector*. France: IEA. https://www.iea.org/reports/net-zero-by-2050.

Grinde, L., H. Heiberg, S. Kristiansen, J. Mamen, R. Gangstø Skaland, and H. T. T. Tajet. 2019. *Vaeret i Norge. Klimatologisk oversikt. Året 2018 [Norwegian weather. Climatological overview of 2018]*. Vaeret i Norge. Oslo, Norway: Norwegian Meteorological Institute.

Hakkaki-Fard, A., P. Eslami-Nejad, Z. Aidoun, and M. Ouzzane. 2015. A techno-economic comparison of a direct expansion ground-source and an air-source heat pump system in Canadian cold climates. *Energy* 87 (July):49–59. doi:gmh44w. doi:10.1016/j.energy.2015.04.093

Holmefjord, V., and A. Kringstad. 2019. *Et elektrisk Norge – fra fossilt til strøm [An electric Norway—from fossil fuels to electricity]*. Oslo, Norway: Statnett.

Kamstrup A/S. 2019. Multical 602 Data Sheet 5810939_N1_GB_09.2019.

Kamstrup A/S. 2021. Temperature Sensors and Pockets Data Sheet 5810337_V1_GB_04.2021.

Kamstrup A/S. 2022. Ultraflow 54 Dn15-125 Data Sheet 58101547_F1_EN_03.2022.

Kouhia, I., J. Nieminen, and R. Holopainen. 2013. *Paroc-passiivitalo: Kylmän ilmaston energiaratkaisu [Paroc passive house—cold-climate energy solution]*. VTT Technology 78. Espoo, Finland: VTT Technical Research Centre of Finland. http://www.vtt.fi/inf/pdf/technology/2013/T78.pdf.

Marszal, A. J., and P. Heiselberg. 2011. Life cycle cost analysis of a multi-storey residential net zero-energy building in Denmark. *Energy* 36 (9):5600–9. doi:fsz8vr. doi:10.1016/j.energy.2011.07.010

Masson-Delmotte, V., P. Zhai, H.-O. Pörtner, D. Roberts, J. Skea, P. R. Shukla, A. Pirani, et al. 2019. *Global warming of 1.5 °C. IPCC Special Report SR15*. Cambridge, UK: Intergovernmental Panel on Climate Change. https://www.ipcc.ch/sr15/.

Midttømme, K., D. Banks, R. K. Ramstad, O. M. Saether, and H. Skarphagen. 2008. Ground-source heat pumps and underground thermal energy storage—energy for the future. In *Geology for Society*, ed. T. Slagstad. Geological Survey of Norway Special Publication 11. Trondheim: Geological Survey of Norway. https://www.ngu.no/en/publikasjon/special-publication-112008-geology-society.

Midttømme, K., M. Justo-Alonso, C. G. Krafft, K. H. Kvalsvik, R. K. Ramstad, and J. Stene. 2021. Geothermal energy use in Norway. Country update for 2015–2019. In *Proceedings World Geothermal Congress 2020*. Reykjavík, Iceland: International Geothermal

Association. https://www.geothermal-energy.org/cpdb/record_detail.php?id=29391.

Norconsult Informasjonssystemer AS, and Bygganalyse AS. 2021. Norsk Prisbok [Norwegian price-book]. https://www.norskprisbok.no/.

Norwegian Meteorological Institute. 2017. Observations and climate data. https://data.norge.no/datasets/8e4414e9-86e7-4661-8775-869474060875.

Norwegian Ministry of Finance. 2021. Prinsipper og krav ved utarbeidelse av samfunnsøkonomiske analyser [Principles and requirements for socioeconomic analyses]. R-109/21. https://www.regjeringen.no/globalassets/upload/fin/vedlegg/okstyring/rundskriv/faste/r_109_2021.pdf.

Norwegian Ministry of Petroleum and Energy. 1990. Lov om produksjon, omforming, overføring, omsetning, fordeling og bruk av energi m.m. https://lovdata.no/dokument/NL/lov/1990-06-29-50.

Paiho, S., S. Pulakka, and A. Knuuti. 2017. Life-cycle cost analyses of heat pump concepts for finnish new nearly zero energy residential buildings. *Energy and Buildings* 150 (September):396–402. doi:gbvjrf. doi:10.1016/j.enbuild.2017.06.034

Pesola, A., M. Autio, J. Alam, L. Ylimäki, L. Descombes, I. Vehviläinen, and J. Vanhanen. 2016. *Energiatehokkaiden malliratkaisujen seuranta ja asukasnäkökulma [Following up energy-efficient model solutions and user perspectives]*. Lahti, Finland: The Housing Finance and Development Centre of Finland. http://hdl.handle.net/10138/159847.

Rad, F. M., A. S. Fung, and W. H. Leong. 2013. Feasibility of combined solar thermal and ground source heat pump systems in cold climate, Canada. *Energy and Buildings* 61 (June):224–32. doi:f47ztb. doi:10.1016/j.enbuild.2013.02.036

Rindal, L. B., and F. Salvesen. 2008. *Solenergi for varmeformål – snart lønnsomt? [Solar thermal energy—soon profitable?]*. Oslo, Norway: Norwegian Water Resources and Energy Directorate.

Ristimäki, M., A. Säynäjoki, J. Heinonen, and S. Junnila. 2013. Combining life-cycle costing and life-cycle assessment for an analysis of a new residential district energy system design. *Energy* 63 (December):168–79. doi:f5nr8v. doi:10.1016/j.energy.2013.10.030

Sidelnikova, M., D. E. Weir, L. H. Groth, K. Nybakke, K. E. Stensby, B. Langseth, J. E. Fonneløp, et al. 2015. *Kostnader i energisektoren. Kraft, varme og effektivisering [Costs in the energy sector. Electricity, heat, and energy efficiency]*. Oslo, Norway: Norwegian Water Resources and Energy Directorate.

Skaland, R. G., H. Colleuille, A. S. H. Andersen, J. Mamen, L. Grinde, H. T. T. Tajet, E. Lundstad, et al., 2019. *Tørkesommeren 2018 [The 2018 summer draught]*. Oslo, Norway: Norwegian Meteorological Institute.

Statistics Norway 2021a. *Electricity balance (MWh)*. Oslo, Norway: Statistics Norway. https://www.ssb.no/en/statbank/table/12824.

Statistics Norway. 2021b. *Consumer price index*. Oslo, Norway: Statistics Norway. https://www.ssb.no/en/statbank/table/08981.

Strand-Hansen, S., and L. Bugge. 2020. Konseptutredning Sandvika sentrum. Enova sluttrapport [Assessment of concepts for Sandvika city centre. Enova final report]. 623336-02. Asplan Viak.

Taylor, J. R. 1997. *An introduction to error analysis: The study of uncertainties in physical measurements*. 2nd ed. Sausalito, CA, USA: University Science Books.

Traaen, K. B. 2018. Bergvarmepumper. Lokale eller kollektive energibrønner [Ground-source heat pumps. Individual or collective boreholes]. Master's thesis, Norwegian University of Life Sciences. http://hdl.handle.net/11250/2565318.

Uthus, B. O., K. Samdal, and F. Trengereid. 1998. *Utbyggingskostnader i hovedfordelings- og fordelingsnettet [Costs of investments in primary and secondary distribution grids]*. Oslo, Norway: Norwegian Water Resources and Energy Directorate.

Weeratunge, H., J. de Hoog, S. Dunstall, G. Narsilio, and S. Halgamuge. 2018. Life-cycle cost optimization of a solar assisted ground-source heat pump system. In *2018 IEEE Power & Energy Society General Meeting (PESGM)*, 1–5. Portland, OR: IEEE. doi:ggdt8m.

Wijst, D. V. D. 2013. *Finance: A quantitative introduction*. Cambridge, UK: Cambridge University Press. https://www.cambridge.org/9781107029224.

World Meteorological Organization. 2017. *WMO guidelines on the calculation of climate normals*. Geneva, Switzerland: WMO-No. 1203.

Wörsdörfer, M., T. Gül, J. Dulac, T. Abergel, C. Delmastro, P. Janoska, K. Lane, and A. Prag. 2019. *Perspectives for the clean energy transition. The critical role of buildings*. France: IEA. https://www.iea.org/reports/the-critical-role-of-buildings.